2014

Experimental Study and Analysis of a Polymer Fiber Bragg Grating Embedded in a Composite Material

Ginu Rajan
Technological University Dublin, ginu.rajan@tudublin.ie

Manjusha Ramakrishnan
Technological University Dublin, manjusha.ramakrishnan@mydit.ie

Yuliya Semenova
Technological University Dublin, yuliya.semenova@tudublin.ie

Eliathamby Ambikairajah
University of New South Wales

Gerald Farrell
Technological University Dublin, gerald.farrell@tudublin.ie

Recommended Citation

Rajan, G. et al. (2014) Experimental Study and Analysis of a Polymer Fiber Bragg Grating Embedded in a Composite Material. *JOURNAL OF LIGHTWAVE TECHNOLOGY,* VOL. 32, NO. 9, MAY 1st. doi:10.1109/JLT.2014.2311441

Experimental Study and Analysis of a Polymer Fiber Bragg Grating Embedded in a Composite Material

Ginu Rajan, Manjusha Ramakrishnan, Yuliya Semenova, Eliathamby Ambikairajah, Gerald Farrell and Gang-Ding Peng

Abstract— **The characteristics of polymer fiber Bragg gratings (FBGs) embedded in composite materials are studied in this paper and are compared with characteristics of their silica counterparts. A polymer FBG of 10 mm length which exhibits a peak reflected wavelength circa 1530 nm is fabricated and characterized for this purpose. A silica FBG with a peak reflected wavelength circa 1553 nm is also embedded in the composite material for a comparison study. The fabricated composite material sample with embedded sensors is subjected to temperature and strain changes and the corresponding effects on the embedded polymer and silica FBGs are studied. The measured temperature sensitivity of the embedded polymer FBG was close to that of the same polymer FBG in free space, while the silica FBG shows elevated temperature sensitivity after embedding. With an increase in temperature, spectral broadening was observed for the embedded polymer FBG due to the stress induced by the thermal expansion of the composite material. From the observed wavelength shift and spectral bandwidth change of the polymer FBG, temperature and thermal expansion effects in the composite material can be measured simultaneously.**

Index Terms— composite materials, polymer fiber Bragg gratings

I. Introduction

COMPOSITE material structures are widely used in the aerospace, marine, aviation and civil engineering industries, because of their advantages of high strength and stiffness with less weight [1-3]. Due to their widespread use, structural health monitoring technologies for composite structures have been studied extensively in order to assess the safety and the durability of the structures. Traditional nondestructive evaluation techniques are effective in detecting damage in materials and structures, but are difficult to use under operational conditions due to the size and weight of the devices [4]. For these reasons fiber optic sensors have been considered as an alternative for in-situ monitoring of composite materials for both the manufacturing process and during service life [5-6].

Among the different fiber optic sensors, the most researched fiber optic sensors for application in composite materials were silica fiber Bragg grating sensors [7-8] and polarimetric fiber sensors [9-10]. However most of the studies were focused on the use of fiber sensors to measure the temperature and strain during the curing process and also during structural tests [7-10]. Our recent studies established that the thermal expansion effects of the composite material considerably affect the performance of the embedded sensors and result in a cross sensitivity in sensing parameters [11-13]. Therefore it is important to differentiate the influence of temperature of the composite material and thermal expansion induced effects on the embedded fiber sensor. It has been reported earlier that FBGs written in micro structured fibers can be used for measurement of temperature and thermally induced strain in the composite materials simultaneously [14-15]. Polarimetric fiber sensors based on polarization maintaining photonic crystal fibers can also be used to measure thermal effects in composite materials [12, 13]. However these approaches involve complex fabrication techniques and instrumentation requirements.

Polymer fiber Bragg gratings (FBG) have attracted much interest among application engineers and scientists due to their unique advantages compared to the silica counterparts, such as the inherent fracture resistance, low Young's modulus, high flexibility, high temperature sensitivity, large strain measurement range, and low density [16-19]. In recent years, advancements in the fabrication of singlemode polymer optical fiber (POF) have also enhanced the research and development of Bragg grating sensors in POF [20]. Sensors for different applications based on singlemode POF gratings have been reported [21-22]. For composite materials, the attractive characteristics of polymer FBGs include their high temperature sensitivity, large strain range and the absence of buffer coating. These distinct features of the polymer FBGs might give an edge over the standard silica FBGs in measuring some of the parameters of the composite materials. Therefore it is worthwhile to explore the possibilities of embedding polymer FBGs in composite materials and also to study the performance of the embedded polymer FBGs compared to their silica counterparts.

In this paper an experimental study to understand the feasibility of using polymer fiber Bragg grating for composite material health monitoring is conducted. For this purpose a singlemode polymer FBG is fabricated and characterized and is then embedded inside a composite material sample, together

G. Rajan, E. Ambikairajah, and G-D. Peng are with School of Electrical Engineering and Telecommunications, The University of New South Wales, Sydney, Australia. Email:- ginu.rajan@unsw.edu.au.

M. Ramakrishnan, Y. Semenova and G. Farrell are with Photonics Research Centre, Dublin Institute of Technology, Dublin, Ireland.

with a reference silica FBG for comparison. The effect of temperature, strain and thermal expansion of the composite material on the polymer and silica fibers are studied and presented in this paper. A major outcome of this study is confirmations of the capability of polymer fiber Bragg gratings for structural health monitoring and related applications. The paper is organized as follows: the fabrication and characterization of the polymer fiber Bragg grating are presented in section II, while in section III, the fabrication of the composite material with embedded fiber sensors is presented. The experimental arrangement for the study is detailed in section IV, and the temperature and strain induced effects are presented in section VI of the paper. Finally discussion and conclusions are presented in Sections VII and VIII respectively.

II. Fabrication and Characterization of Polymer Fiber Bragg Gratings

A. *Singlemode Polymer Fiber*

The photosensitive singlemode polymer fiber used in this study is fabricated in-house and the fabrication procedure for the poly(methyl methacrylate)(PMMA)-based POF used in this work is explained in [23-25]. The difference in the refractive index between the core and cladding was 0.0086. The POF fiber sample used in this study had an outer diameter of ~240-260 µm and a 12 µm core diameter and the fiber was single mode at the wavelength of operation.

B. *POF Grating Fabrication*

The Bragg grating structures are fabricated in the polymer fibers by phase mask technique using a 50 mW continuous wave Kimmon IK series He-Cd Laser emitting light at 325 nm [21]. The laser beam was irradiated onto the side of the polymer fiber through the phase mask placed parallel to the fiber. The phase mask was 10 mm long and had a pitch of 1030 nm which was designed for an irradiation wavelength of 320 nm and to produce 10 mm long gratings with a peak reflected wavelength of approximately 1530 nm in the POF used in this experiment. Two plano-convex cylindrical lenses were also used in the setup, one to expand the beam to cover approximately 10 mm of the fiber and the other one with a focal length of 30 mm to focus the expanded beam to the core region of the POF. An XYZ translation stage is used to adjust the position of the fiber to so that, the UV light is uniformly focused on the core of the polymer fiber. The experimental arrangement to fabricate the polymer FBG is shown in Fig 1.

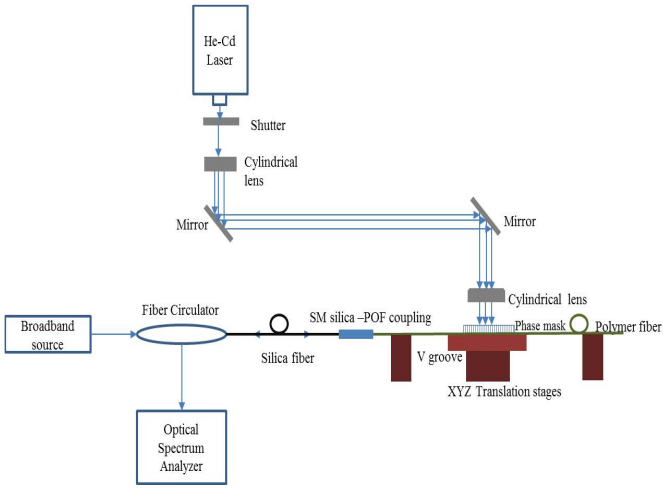

Fig.1. Schematic of the experimental setup to fabricate polymer fiber Bragg gratings.

A short length POF of approximately 12 cm is used with the grating inscribed in the middle region of the fiber and the polymer fiber is glued to a silica singlemode fiber pigtail using a UV curable glue [26]. Due to the available experimental setup to fabricate gratings at the C band, and due to the loss of the polymer fiber in this wavelength band, short length of polymer fibers (12 cm) are used. To observe the FBG reflection spectrum, a high power broadband source with a range of 1520-1590 nm with peak power at 1530 nm is used as the input light source and the reflected spectrum is directed via a fiber circulator to the optical spectrum analyzer and is then monitored and recorded. The observed reflectivity of the fabricated gratings was approximately 40%.

C. *POF Grating Characterization*

The fabricated polymer FBG was characterized for strain and temperature. Strain with values of up to 2000 µε is applied to the fiber with a step change of approximately 200 µε. This is carried out by fixing the ends of the polymer fibers on translation stages and by applying a fixed step translation. The elongation of the polymer fiber is limited to less than 1 % to make sure that there are no hysteresis effects [27] and in our experiments within the applied strain range no significant hysteresis was found. The measured Bragg wavelength shift for the applied strain is shown in Fig 2(a). The strain sensitivity of the polymer FBG calculated from the measured data is approximately 1.34 pm/µε. This value is slightly higher than the strain sensitivity of silica FBG, which is normally 1.2 pm/µε at 1550 nm.

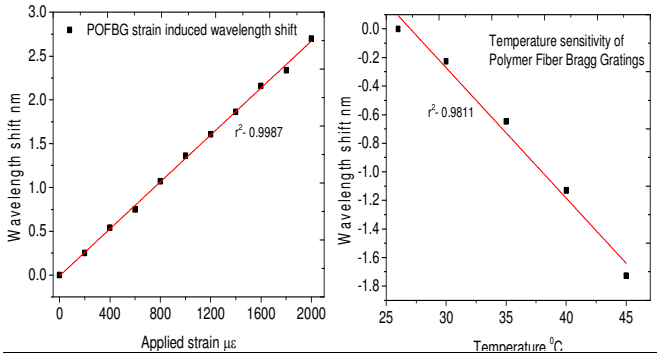

Fig. 2. Measured Bragg wavelength shift for the polymer FBG (a) with change in strain (b) with change in temperature.

To measure the temperature sensitivity of the polymer FBG, the sensor is placed on a hotplate, controlled by a temperature controller, which has an accuracy of ±0.1 ^{0}C. The temperature of the polymer FBG is varied from 25 ^{0}C to 45 ^{0}C with a step change of 5 ^{0}C and the corresponding wavelength shifts were measured. Due to the negative thermo- optic coefficient of the polymer fiber, a blue shift in the Bragg wavelength was observed and the measured wavelength change is shown in Fig 2(b). The calculated temperature

sensitivity of the polymer FBG dervied from the results is 90 pm/^{0}C. This temperature sensitivity is almost 8 times higher than that of a typical silica FBG, which is approximately 11.2 pm/^{0}C. This high temperature sensitivity characteristic property of the polymer FBG will make it ideal to study temperature effects in composite materials.

III. Fabrication of Composite Material Sample with Embedded FBGs

The composite material sample is fabricated by using a hand lay-up method with glass fibre fabrics (E-glass) as the reinforcement and a general purpose unsaturated polyester resin as the matrix material [11-13]. The orientations of the glass fibres were unidirectional (0/0) to each other. The matrix material is prepared from the polyester resin with a catalyst added to the resin at a rate of 1% by volume. The reinforcement glass woven fabric with a density of 280 g/m^2 is cut into 8 pieces with dimensions of 10 cm x 5 cm.

The fabricated composite sample has 8 plies with the fiber gratings placed in the 2nd layer. To allow a comparison study, a 10 mm long silica FBG with a peak reflected wavelength circa 1553 nm is also embedded into the composite together with the polymer FBG. A schematic of the cross section of the composite material with embedded fiber sensors is shown in Fig 3(a). Careful consideration has been given to placing of the optical fiber sensors in the composite layer. FBG sensors are placed adjacently 1 mm apart from each other in the middle region of glass fabric, approximately 5 cm from both ends. Before embedding within the composite, pre-strain was applied to the fiber by fixing both ends of the fibers on a translation stage and applying translation using the linear stages. The 2nd layer is chosen as the host layer for the optical fibers in order to reduce the risk of breakage of the polymer and silica fiber Bragg gratings and also to increase the strain and temperature effects as the outer most layers (layer 1) will experience these effects at the highest level. In the present experiment, layer 1 will be in contact with the heat source for temperature studies and while applying strain, the upper outer layer (layer 1) will experience the maximum tensile strain and lower outer layer (layer 8) will experience the maximum compressive strain. The sample is cured as per the manufacturer's specifications at room temperature for three days. The thickness of the cured composite sample was 2.1 mm. A photograph of the fabricated sample is shown in Fig 3(b).

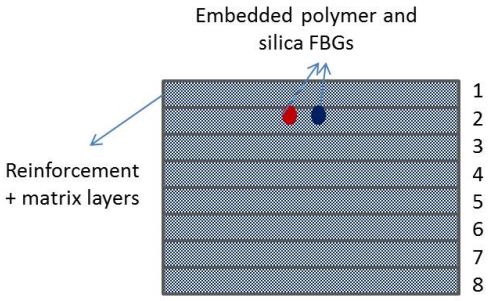

(a)

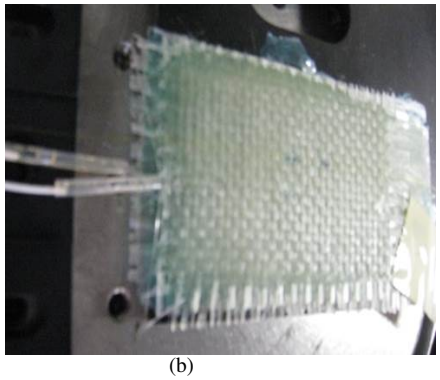

(b)

Fig. 3. (a) Schematic of the cross section of the composite material with embedded sensors (c) Photograph of the cured composite material with embedded FBGs.

The spectral responses of the polymer and silica FBGs are also measured before and after embedding. The polymer FBG shows some changes in its spectral shape and amplitude after embedding. This may be due to the stress induced on the fiber during the curing process. The measured reflection spectra of the polymer FBG before and after embedding are shown in Fig 4. The noise level of the grating's reflected spectrum also changed with some ripples appearing and it is believed that this could be due to the small distortions arisng in the glued polymer-silica region while embedding the fiber. The silica FBG does not show any significant changes in its reflected spectrum after embedding in the composite material.

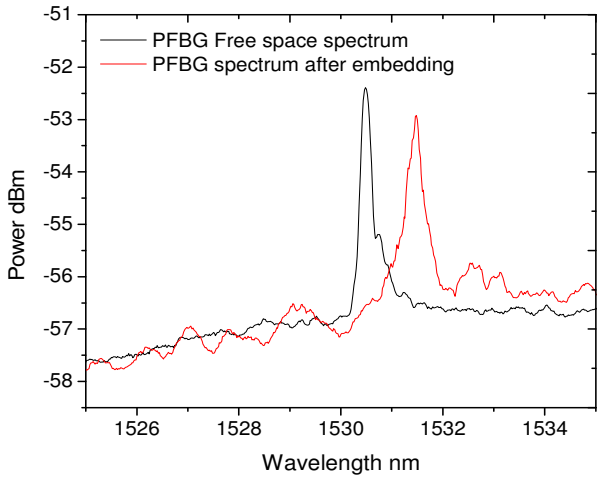

Fig. 4. Measured spectrum of the polymer FBG before and after embedding inside the composite material.

IV. Experimental Arrangement to Study the Temperature and Strain Effects on the Embedded FBG

To study the thermal behavior of the embedded polymer FBG sensors, the composite material sample is placed on a hotplate controlled by a temperature controller. A temperature range from 25 ^{0}C to 50 ^{0}C can be obtained by the setup with a temperature accuracy of ±0.1 ^{0}C. The temperature of the composite material sample is initially set at 25 ^{0}C and increased up to 45 ^{0}C with an incremental step change of 5 ^{0}C. For each step a 5 minute interval is allowed for to make sure the temperature is uniformly distributed across the sample. The experimental setup for thermal study is shown in Fig 5(a).

For applying strain to the composite material sample with

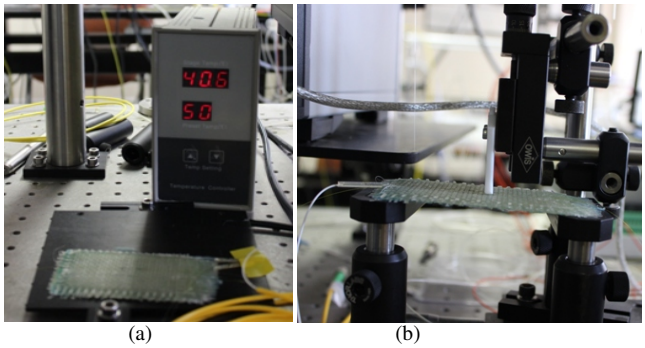

(a) (b)

Fig. 5. (a) Experimental setup to apply temperature changes to the composite material (b) Experimental arrangement to apply strain to the composite material sample.

embedded FBGs, a 3-point bending setup is adopted, where the two long ends of the composite material are placed on two rigid supports and the load is applied to the middle of the sample, as shown in Fig 5(b). In this case the outer region of the composite sample will experience a tensile strain and the inner surface will experience a compressive strain. The sample is orientated in such a way that tensile force is exerted on the embedded FBG. The strain induced in the different layers of the composite material sample can be calculated analytically using the following formula [28]:

$$\varepsilon = 6\frac{sd}{L^2}\,, \qquad (1)$$

where s is the deflection at the centre, d is the distance between the fiber layers and L is the length of the sample. Using this equation the peak strain in the 2nd layer of the composite material sample calculated for a 2.5 mm deflection is 2795 με. For a 3-point bending scheme the composite material experiences a non-uniform strain across its length with maximum strain experienced in the middle region and minimum at the edges. Since the FBG is placed in the centre of the sample and covers 1 cm of the total length of the sample, the estimated average strain at the 1 cm region in the middle of the sample is approximately 60% of the maximum strain [11].

V. Temperature and Strain Induced Effects on the Embedded Polymer FBG and Its Comparison with a Silica FBG

For an FBG sensor embedded inside a composite material, three effects can take place due to change in temperature: (i) wavelength shift induced by the thermo-optic effect and thermal expansion of the polymer fiber; (ii) wavelength shift induced by a longitudinal strain resulting from the thermal expansion of the composite sample; (iii) wavelength shift and spectral broadening corresponding to a transverse strain (or thermal stress) induced by thermal expansion of the composite sample. Due to the combined effect of (i) and (ii) the temperature sensitivity for the embedded FBG sensor will be different from that for a free space grating and if the transverse strain is effectively transferred to the grating, additionally a spectral broadening can be observed. Based on the type of reinforcement used, orientation of the reinforcement ply and matrix materials, the magnitude of the wavelength shift due to thermal expansion may vary. The values of strain components acting upon the optical fiber in different directions also depend on the orientation of the reinforcement fibre ply.

Considering only the temperature effect on the FBG and the thermal expansion induced mechanical strain, the net wavelength shift for an embedded FBG with temperature can be written as;

$$\Delta\lambda_T = \left(\alpha + \xi + k_c\right)\lambda_B \Delta T\,, \qquad (2)$$

where α is the coefficient of the thermal expansion (CTE) and ζ is the thermo-optic coefficient of the optical fiber respectively. λ_B is Bragg wavelength of the FBG. The coefficient k_c corresponds to the effective mechanical strain on the FBG due to the thermal expansion of the composite material.

Considering only the effect of longitudinal strain applied to the FBG, the strain induced wavelength shift $\Delta\lambda_S$ for the embedded FBG can be written as;

$$\Delta\lambda_S = \lambda_B(1-\rho_\alpha)\Delta\varepsilon\,, \qquad (3)$$

where ρ_α is the effective strain-optic constant of the optical fiber.

In order to understand the magnitude of the effect of thermal expansion of the composite material on the embedded FBG, one must evaluate the coefficients of thermal expansion in both longitudinal and transverse directions for the type of the composite material used for embedding. In this work an E-glass reinforcement- unsaturated polyester resin matrix combination is used to fabricate the composite material sample. The sections below present the thermal behavior of E-glass composites and their influence on the embedded polymer and silica FBG sensors.

A. Thermal Behavior of E-Glass Composites

The thermal behavior of composite materials can be predicted from the elastic and thermal properties of reinforcement fibers and the matrix material. For the modeling of the thermal expansion coefficients, the values of the mechanical properties of the reinforcement fibers/matrices are obtained from the manufacturer's data sheet together with the fiber volume fraction obtained from the Thermo Gravimetric Analysis(TGA) measurements and are presented in Table 1(a) and 1(b) respectively for the reinforcement and the matrix material. E, α and υ represents the elastic modulus, thermal expansion coefficient and poison ratio of the materials respectively. Indices f, m, represents reinforcement fibre and matrix materials, and l and t denotes longitudinal and transverse directions respectively. From TGA the fiber volume fraction, V_f value of E-glass composite is estimated to be 0.47. The thermal expansion coefficient calculations are carried out using a Classical Laminate Theory (CLT) based composite analysis Matlab tool [29, 30].

Fibre type	E_{lf} (Gpa)	E_{tf} (Gpa)	υ_{12}	α_{lf} x 10^{-7} (m/m/^{0}C)	α_{tf} x 10^{-5} (m/m/^{0}C)
E glass	72.4	72.3	0.28	5.40	1.00

Table 1(a). The physical properties of E-glass reinforcement fibre

Composite material	Physical properties of Matrix				Fibre volume fraction V_f
	E_m (Gpa)	υ_m	α_m x 10^{-5} (m/m/^{0}C)	V_m	
E glass-Unsaturated polyester	4.6	0.36	3.08	0.53	0.47

Table 1(b). The physical properties of reinforcement matrix

In composite materials the elongations due to thermal expansion are characterized by the two coefficients of thermal expansion, longitudinal CTE and transverse CTE. In the direction of the reinforcement fibers, the contribution to the thermal expansion is dominated by the reinforcement fibers, and in the direction perpendicular to the reinforcement fibers, the contribution to the thermal expansion is dominated by the matrix material [31, 32]. The theoretically estimated thermal expansion coefficients of the composite specimen are listed in Table 2.

Material	Theoretical thermal expansion coefficients	
	Longitudinal CTE α_l x 10^{-6} (m/m/^{0}C)	Transverse CTE α_t x 10^{-5} (m/m/^{0}C)
E glass-Unsaturated polyester	0.145	2.678

Table 2. Theoretical prediction of the thermal expansion coefficients of composite samples calculated by Classical Laminate Theory

From Table 2 it can be seen that for the E-glass- unsaturated polyester resin composite material, the transverse CTE is significantly higher compared to the longitudinal CTE and can induce higher stress on the embedded optical fiber than longitudinal strain with a change in temperature. This characteristic property of the composite material also points out the complexity involved in measuring the real temperature of composite materials using embedded fiber sensors and also the importance of measuring and differentiating between the thermal expansion induced stress and applied mechanical strain, in order to achieve an accurate and complete characterization of composite materials.

B. Thermal Stress and Strain Effects on the Embedded Sensors

To study the temperature induced effects on the embedded polymer FBG, first the reflected spectra of the embedded polymer FBG are measured at different temperatures from 25 ^{0}C to 45 ^{0}C at 5 ^{0}C temperature intervals as shown in Fig 6(a). From the figure it can be seen that for the polymer FBG, the reflected spectrum broadens and distorts with multiple peaks starting to appear as the temperature increases. For comparison the reflected spectra of the embedded silica FBG are also measured at the same temperatures and are shown in Fig 6(b). In the case of silica FBG, a small spectral peak distortion is noticeable but no significant spectral broadening is observed.

The wavelength shifts observed for the polymer FBG and silica FBG are also measured and shown in Fig 7(a). From the figure it can be seen that a blue shift is observed for the polymer FBG due to the negative thermo optic coefficient, while a red shift is observed for the silica FBG. The observed temperature sensitivity of the embedded polymer FBG is 92.28 pm/^{0}C which is close to the free space temperature sensitivity of 90 pm/^{0}C.

Due to the fact that for a polymer FBG strain and temperature effects result in Bragg wavelength shifts in opposite directions, it was expected that for the polymer FBG embedded in E-glass composite subjected to thermal strain and stress the overall Bragg wavelength shift should be small. However this expectation was not confirmed in our experiment. One likely explanation is that in the case of polymer fiber the longitudinal thermal strain is not effectively transferred to the polymer FBG.

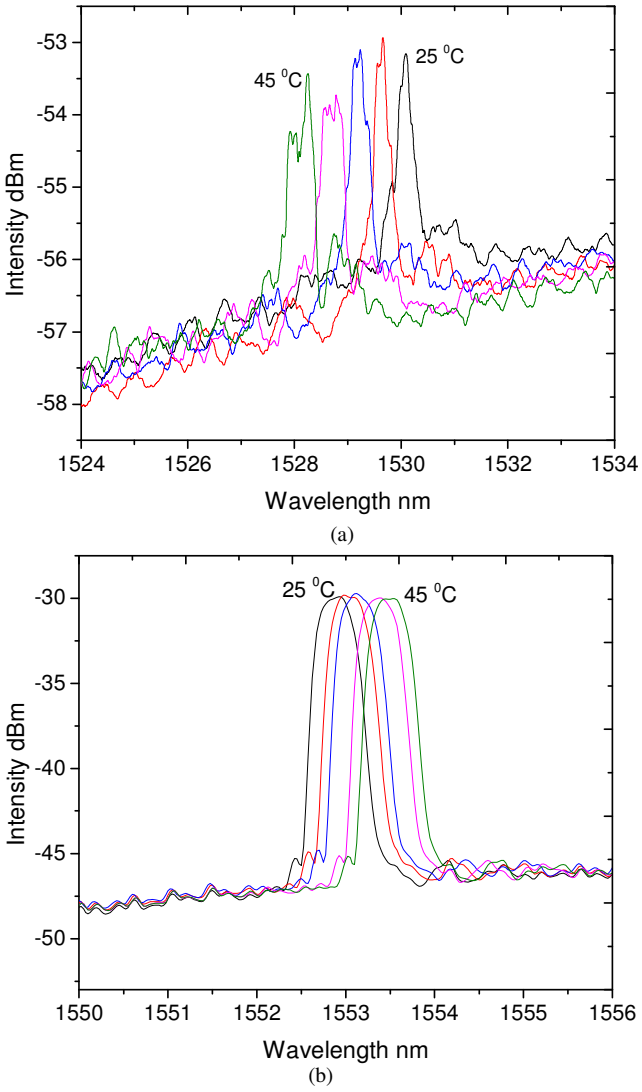

Fig. 6. Reflection spectra at different temperatures (a) Polymer FBG (b) Silica FBG.

On the other hand, the effects of thermal stress/transverse strain on the embedded polymer FBG are evident through the form of spectral broadening observed in Fig 6(a). In order to quantify the effect of broadening, the change in bandwidth of the reflection spectra of the polymer FBG is measured at different temperatures. The measured 1.5 dB bandwidth of the

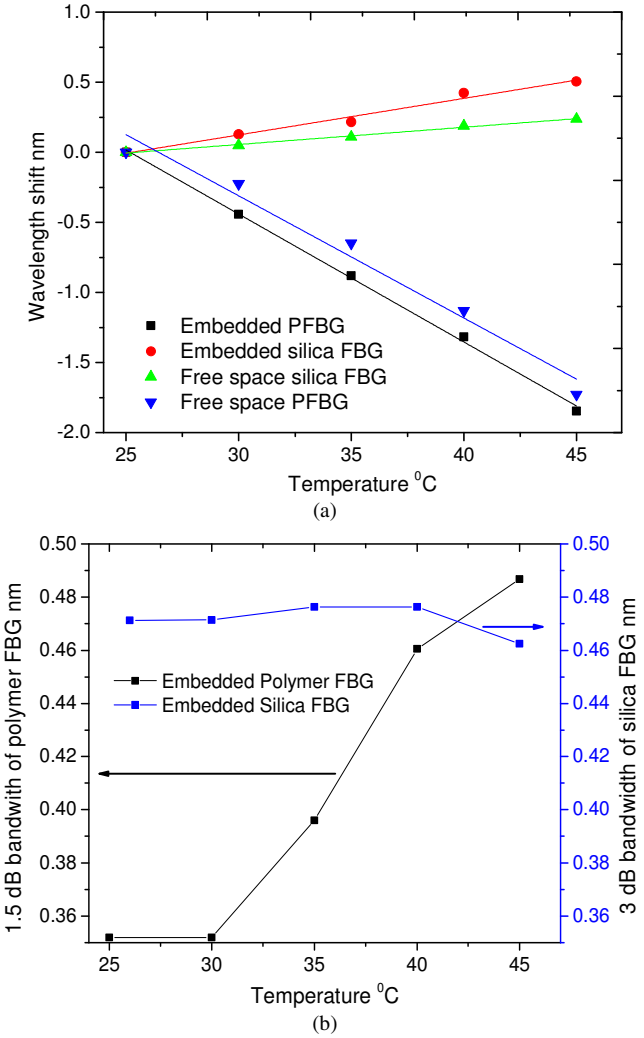

Fig. 7. (a) Temperature induced wavelength shift of the embedded polymer and silica FBGs and its comparison with free space FBGs (b) Measured 1.5 dB bandwidth of polymer FBG and 3 dB bandwidth of silica FBG at different temperatures.

polymer FBG is shown in Fig 7(b) and it can be seen that the bandwidth increases as the temperature increases. The 1.5 dB bandwidth is used instead of the 3 dB bandwidth due to the fact that for a polymer FBG the noise floor is relatively high because of coupling related issues and the 3 dB bandwidth could not be reliably measured. The measured bandwidth change for the embedded polymer FBG within the temperature range of 30-45 ^{0}C was 8.5 pm/^{0}C. Therefore from the observed spectral broadening and distortion, it can be concluded that the thermal expansion induced stress is effectively transferred to the polymer fiber and can be measured using a polymer FBG. It is assumed that the reason for this is the absence of a buffer coating for the polymer fiber, which results a direct transfer of the surrounding physical phenomena directly to the core and cladding of the polymer fiber. Stress induced by localized micro-bends in the composite material could also contributes to the chirping effect seen in Fig 6(a).

In the case of the silica FBG, an elevated temperature sensitivity of 25 pm/^{0}C is observed after embedding compared to the free space sensitivity of 11.2 pm/^{0}C which is also shown in Fig 7(a). This means that the thermal expansion induced mechanical strain contributes towards the overall temperature sensitivity of the embedded silica FBG. From the theoretical estimation for a temperature change of 20 ^{0}C, the expected longitudinal strain due to thermal expansion is only 2.3 με (0.145 με/^{0}C) which corresponds to a wavelength change of 2.76 pm. Therefore the measured additional wavelength shift of 13.8 pm/^{0}C is assumed to be due to the influence of high thermal stress/transverse strain (26.8 με/^{0}C), where some components of the stress/strain act in the direction of the optical fiber due to the inhomogeneous nature of the composite material. However for the silica FBG, the 3dB bandwidth remains constant, as no spectral broadening is observed as shown in Fig 7(b). This implies that the thermal stress/strain in the transverse direction is not directly transferred to the silica core/cladding of the fiber as it is absorbed by the polymer buffer coating and also no localized strain gradient has occurred in the composite material. Therefore the observed elevated temperature sensitivity possibly originates from the components of the transverse stress/strain acting in the direction of the optical fiber.

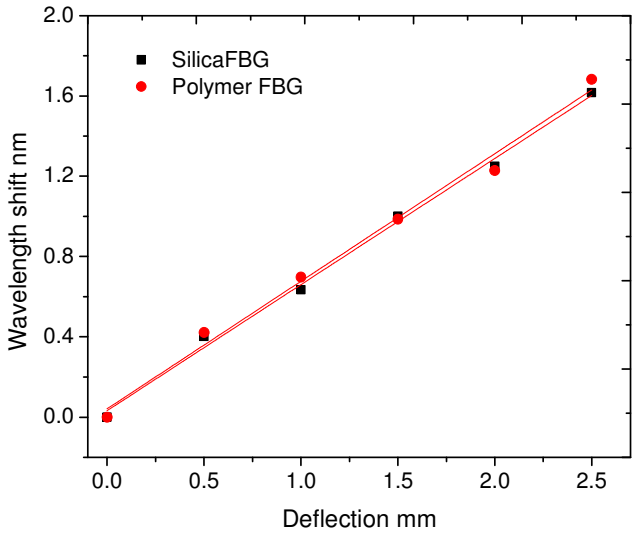

Fig. 8. Measured wavelength shifts of the polymer and silica FBGs with deflection in the middle of the composite material.

C. *Strain Induced Effects*

In order to measure the strain sensitivity of the embedded FBGs, loads are applied to the middle region of the composite material sample and the effects of the induced strain on the embedded polymer and silica FBG are measured. Deflections up to 2.5 mm are applied to the sample and the measured wavelength shifts for both silica and polymer FBGs are shown in Fig 8. No spectral distortions are observed for both polymer and silica FBGs. From the figure it can be seen that the measured strain sensitivity of the embedded polymer and silica FBGs are very close to each other. In free space the polymer FBG had a slightly higher strain sensitivity (1.34 pm/με) compared to that of silica FBG (1.2 pm/με). The similarity in the measured strain sensivity of the embedded silica and polymer FBGs underlines the fact that longitudinal strain in the composite is not effectively transferred to the polymer fiber. For a fiber embedded in the 2nd layer, the estimated average strain in the 1 cm long middle region was approximately in the range of 1677 με for a 2.5 mm

deflection. For the silica FBG, assuming a 1.2 pm/με, a wavelength shift of 1.7 nm corresponds to a strain value of 1416 με which is close to the estimated value. This confirms, that the silica FBG is measuring the strain values correctly. However for the polymer FBG, with a strain sensitivity of 1.34 pm/mε, a wavelength shift of 1.9 nm was expected, but the measured value was only 1.7 nm which gives a strain value of 1268 με. The discepency in the measured strain values can be attributed to the differnces in mechanical properties of the polymer fiber and the composite material which resulted in the mechanical strain not being effectively transferred to the polymer FBGs as compared to the case of silica FBG.

VI. Discussion

For E-glass fiber based composites, which is one of the most commonly used types of composite materials, our analysis has demonstrated that transverse CTE is very high compared to longitudinal CTE. This means that it is more important to measure transverse thermal effects than longitudinal thermal effects. However in order to do so one might require a sensor which can measure the temperature and stress simultaneously. From the results shown in section V it can be seen that the polymer FBGs are sensitive to thermal stress and are less sensitive to longitudinal strain induced by temperature. Since in the case of E-glass-polyester resin composite material, transverse CTE is more prominent, the change in bandwidth of the polymer FBG can be taken as an indication of thermal expansion of the composite material and the peak wavelength shift can be taken as a measure of temperature change. The difference between the measured temperature sensitivity of the embedded polymer FBG and the free space polymer FBG was only 2.2 pm/^{0}C. Given the very high temperature sensitivity of the polymer fiber grating, this can only contribute a small error in the measured temperature in the range of ± 0.025 ^{0}C. This minor temperature error can be disregarded in most of cases. Therefore given the very small cross talk between the temperature sensitivity and the thermal strain induced sensitivity, from the measured spectral wavelength shift and the change in spectral bandwidth, it can be reasonably assumed as an indicative measure of temperature and thermal expansion of composite material. A summary of the observed phenomena given in Table 3, shows the ability of both polymer and silica FBGs' capacity to measure temperature induced effects in composite materials. From the results obtained from the embedded polymer FBG it can be concluded that with an appropriate calibration, the temperature and thermal expansion of the composite can be measured using the same fiber sensor.

FBG type	Temperature sensitivity @ Free space pm/^{0}C	Temperature Sensitivity @ embedded pm/^{0}C	Thermal expansion induced wavelength shift pm/^{0}C	Bandwidth change @ embedded pm/^{0}C
Silica	11.2	25	13.8	0
Polymer	90	92.28	2.28	8.5

Table 3. Measured sensitivities of the polymer and silica FBGs

The silica FBG is also sensitive to the thermal expansion of the composite material as it has shown elevated temperature sensitivity once embedded within the composite material. However to extract the thermal expansion information of the composite material from the silica FBG's wavelength shift, an additional source of temperature information is required, due to the cross sensitivity between temperature and other thermal induced effects. Therefore using standard silica FBGs, it is not possible to simultaneously measure both the thermal expansion of the composite material and temperature simultaneously, and such a measurement might require gratings inscribed in special fibers such as micro-structured or highly-birefringent fibers. Therefore polymer FBGs might be a better option for composite material to measure temperature and temperature induced effects within the working temperature range of both the polymer grating and the composite materials.

For the completion of the composite material characterization, the sample was subjected to external strain and corresponding shifts in wavelengths for both silica and polymer FBGs were measured and presented in section V(C). From the results it was observed that both silica and polymer FBGs have shown the same strain sensitivity in the embedded state, which implies that the polymer FBG is not efficiently measuring the applied strain, and therefore a silica FBG would be a better candidate to accurately measure strain in composite materials.

Although the polymer FBG is capable of measuring both temperature and thermal expansion effects in the composite material, it also suffers from some shortcomings. One issue that is not discussed in this paper is the humidity sensitivity of the polymer FBG. The humidity sensitivity of the FBG fabricated from the same type of polymer fiber used in this experiment is presented in ref 22 and ref 33. In this experiment humidity has less influence on the embedded sensor because of two reasons; firstly, the embedded sensor is almost saturated for humidity. Secondly, the response time of polymer fiber grating to humidity is very slow, compared to the effects of temperature. Due to these reasons, it is assumed that, temperature induced humidity change has negligible influence on the temperature studies presented in this paper. Some of the limitations of the of the polymer fiber Bragg gratings are high transmission loss and coupling issues. Inscribing gratings which exhibit a lower peak reflected wavelength [34] could improve the overall power budget of the system and longer length POFs can be embedded in the composite material compared to those used in this study. Another short coming of the POF based sensors is its working temperature range. Most of the polymer grating sensors would only work up to a temperature range of 80 ^{0}C. But for composite materials, curing can be done within this temperature range, but for high temperature applications POF grating may not be a good alternative. Another issue with singlemode POF sensors is the coupling issue. A stable coupling method for polymer fibers is proposed by the authors [26], however further studies on the long term stability of coupling are yet to be conducted.

VII. CONCLUSION

Composite materials with embedded polymer fiber Bragg gratings were fabricated and the characteristic properties of the embedded polymer FBG were studied and compared with those of an embedded silica FBG. The composite material sample with embedded FBGs was subjected to temperature and strain changes and the corresponding effects on the embedded polymer FBG and silica FBG were studied. For the polymer FBG spectral broadening was observed due to the thermal expansion of the composite, but the sensitivity of the embedded polymer FBG to temperature remains the same as that of the free space polymer FBG. With appropriate calibration, the temperature and thermal expansion of the composite can be measured using the embedded polymer FBG. The silica FBG shows elevated temperature sensitivity due to the thermal expansion of the composite, but requires additional temperature information to measure temperature and thermal expansion simultaneously. By improving the transmission loss and coupling issues polymer FBG might be a good candidate for sensing solutions for composite materials.

ACKNOWLEDGEMENTS

GR wishes to acknowledge the support through the UNSW Vice-Chancellors Research Fellowship

REFERENCES

[1] Chung, D. D. L., “Composite Materials: Science and Applications,” 2nd Edition, Springer Publications, 2010.

[2] Kim, J. K., Wo, D. Z., Zhou, L. M., Huang, H. T., Lau, and Wang, M., “Advances in Composite Materials and Structures, ” Key Engineering Materials, Vol. 334-335, 2007.

[3] Deo, R. B., Starnes, J. H., and Holzwarth, R. C., “Low-Cost Composite Materials and Structures for Aircraft Applications, ” RTO AVT Specialists Meeting on Low Cost Composite Strcutures, Norway, 2001.

[4] Reid, S. R., “Impact Behaviour of Fibre-Reinforced Composite Materials and Strcutures,” CRC Press, 2003.

[5] Gros, X. E., “Current and Future Trends in Non-Destructive testing of Composite Materials,", Ann. Chim. Sci. Mat, Vol 25, pp. 539-544, 2000.

[6] Garg, D. P., Zikry, M. A., Anderson, G. L., Gros, X. E., “Current and potential future research activities in adaptive structures: an ARO perspective," Smart Mater. Struct. , Vol 10, pp. 610-623, 2001.

[7] Dewynter-Marty, V., Ferdinand, P., "Embedded fiber Bragg grating sensors for industrial composite cure monitoring," Journal of Intelligent Materials Systems and Structures, Vol. 9, pp 785-787, 1998.

[8] Fan, Y., Kahrizi, M., “Characterization of a FBG strain gage array embedded in composite structure,” Sensors and Actuators A, Vol 121, pp. 297-305, 2005.

[9] Murukeshan, V. M., Chan, P. Y., Seng, O. L., and Asundi, A., "On-line health monitoring of smart composite structures using fiber polarimetric sensor," Smart Mater. Struct. , Vol 8, pp. 544-548, 1999.

[10] Hegde, Asundi, A., "Performance analysis of all-fiber polarimetric strain sensor for composites structural health monitoring", NDT&E International, Vol 39, pp. 320-327, 2007.

[11] Rajan. G, Ramakrishnan. M, Lesiak. P, Semenova. Y, Boczkowska. A, and Woliński1. T., and Farrell. G, "Composite materials with embedded photonic crystal fiber interferometric sensors", Sensors and Actuators A: Physical, Vol. 182, pp 57-67, Aug 2012.

[12] Ramakrishnan. M, Rajan. G, Semenova. Y, Boczkowska. A, Domanski. A., Woliński1. T., and Farrell. G, "Influence of thermal expansion of a composite material on embedded polarimetric fiber sensors", Smart Materials and Structures, Vol. 20, No. 12, 2011

[13] Ramakrishnan. M, Rajan. G, Semenova. Y, Boczkowska. A, Domanski. A., Woliński1. T., and Farrell. G, “Measurement of Thermal Elongation Induced Strain of a Composite Material Using a Polarization Maintaining Photonic Crystal Fiber Sensor", Sensors and Actuators A, Vol 190, pp. 44-51, 2013.

[14] Sulejmani, S., et al., “Towards micro-structured optical fiber sensors for transverse strain sensing in smart composite materials” Proc. Sensors 2011 Conf., IEEE, pp 109-112, 2011.

[15] Geernaert, T., et al., “Transversal Load Sensing With Fiber Bragg Gratings in Microstructured Optical Fibers”, IEEE Photonics Technology Letters, Vol 21, No. 1, pp 6-8, 2009.

[16] Peng, G-D., Xiong, Z., and Chu, P.L, "Photosensitivity and Gratings in Dye-Doped Polymer Optical Fibers," Opt. Fiber Technol., vol. 5, pp. 242-251, 1999.

[17] Xiong, Z., Peng,G-D., Wu, B., and Chu, P.L., "Highly Tunable Bragg Gratings in Single-Mode Polymer Optical Fibers," IEEE Photon. Tech. Lett., vol. 11, pp. 352-354, 1999.

[18] Webb, D. J., Kalli, K., Zhang, C., Johnson, I., Chen, FG. X., Rodriguez, D. S., Barton, J. D., Ye, C., Peng, G-D., Argyros A., and Large, M. C. J., "Applications of Polymer Fibre Grating Sensors," The 18th International Conference on Plastic Optical Fibers, September 9-11, 2009.

[19] Kuang, K. S. C., Quek, S. T., Koh, C. G., Cantwell, W. J., and Scully, P. J., "Plastic Optical Fibre Sensors for Structural Health Monitoring: A Review of Recent Progress," J. Sensors, Vol. 2009, 312053, 2009.

[20] Webb, D. J., "Polymer Optical Fibre Bragg Gratings," in Bragg Gratings, Photosensitivity and Poling in Glass Waveguides, OSA Technical Digest, paper Btu3E.4.4, 2012.

[21] Kalli, K., Dobb, H. L., Webb, D. J., Carroll, K., Themistos, C., M. Komodromos, M., Peng, G-D., Fang, Q., and Boyd, I. W., "Development of an electrically tuneable Bragg grating filter in polymer optical fibre operating at 1.55 μm," Meas. Sci. Technol., vol. 17, pp. 3155-3164, 2007.

[22] Zhang, W., Webb, D. J., and Peng, G-D., "Investigation in to Time Response of Polymer Fiber Bragg Grating Based Humidity Sensors," J. Lightwave Technol., vol. 30, pp. 1090-1096, 2012.

[23] Peng, G-D., Chu, P. L., Lou, X., and Chaplin, R. A., "Fabrication and Characterization of Polymer Optical Fibers," J. Electr. Electron. Eng. Aust., pp.289-296, 1995.

[24] Liu, H. Y., Peng, G-D., and Chu, P.L., "Polymer Fiber Bragg Gratings with 28-dB Transmission Rejection," IEEE Photon. Tech. Lett., vol. 14, pp. 935-357, 2002.

[25] Peng, G., Chu, P, L., “Polymer optical fiber photosensitivities and highly tunable fiber gratings”, Fiber and Integrated Optics, vol. 19, pp. 277 – 293, 2000.

[26] Rajan. G, Liu. B, Luo. Y, Ambikiarajah. E, and Peng. G-D, "High sensitivity force and pressure measurements using etched singlemode polymer fiber Bragg gratings", IEEE Sensors Journal, accepted for publication, Jan 2013

[27] Abang, A., Webb, D. J., "Influence of mounting on the hysteresis of polymer fiber Bragg grating strain sensors," Opt. Lett., Vol. 38, No. 9, pp 1376-1378, 2013.

[28] Domanski, A. W., etal., “Comparison of Bragg and Polarimetric Optical fiber Sensors for Stress Monitoring in Composite Materials," Acta Physica Polonica, Vol 116, 2009.

[29] Karadeniz, Z. H., D. Kumlutas, D., "A numerical study on the coefficients of thermal expansion of fiber reinforced composite materials", Composite Structures, 78, 1-10, 2007.

[30] Rich, R, Le., and Gaudin, J., "Design of dimensionally stable composites by evolutionary optimization," Compos. Struct, vol. 41, pp. 97-111, 1998.

[31] Chamis, C.C., "Simplified Composite Micromechanics Equations for Hygral, Thermal and Mechanical properties," SAMPE Quarterly, Vol. 15, pp . 14-23, April 1984.

[32] Deng, X., Chawla, N., “Three-dimensional (3D) modeling of the thermoelastic behavior of woven glass fiber-reinforced resin matrix composites’, J Mater Sci, Vol. 43, Issue 19, pp. 6468-6472, 2008.

[33] Rajan, G., Noor, Y,M., Ambikairajah, E., Peng, G-D., Liu, B., Webb, D, J., “A fast response intrinsic humidity sensor based on an etched singlemode polymer fiber Bragg grating”, Sensors and Actuators A: Physical, vol. 203, pp. 107-111, 2013.

[34] Zhang, Z. F., Zhang, C., Tao, X. M., Wang, G. F., and Peng,G-D., “Inscription of Polymer Optical Fiber Bragg Grating at 962 nm and its Potential in Strain Sensing”, IEEE Photon. Tech. Lett., Vol 22, No. 21, pp. 1562-1564, 2010.